THE JOURNAL OF BIOLOGICAL CHEMISTRY
Vol. 279, No. 28, Issue of July 9, pp. 29572–29582, 2004

Printed in U.S.A.

pH Dependence of Tryptophan Synthase Catalytic Mechanism

I. THE FIRST STAGE, THE β-ELIMINATION REACTION*

Received for publication, February 20, 2004, and in revised form, April 15, 2004
Published, JBC Papers in Press, April 26, 2004, DOI 10.1074/jbc.M401895200

Francesca Schiaretti‡, Stefano Bettati§¶, Cristiano Viappiani¶‖, and Andrea Mozzarelli‡¶**

From the ‡Department of Biochemistry and Molecular Biology, the §Department of Public Health, the ‖Department of Physics, ¶National Institute for the Physics of Matter, University of Parma, 43100 Parma, Italy

The pyridoxal 5′-phosphate-dependent β-subunit of the tryptophan synthase $\alpha_2\beta_2$ complex catalyzes the condensation of L-serine with indole to form L-tryptophan. The first stage of the reaction is a β-elimination that involves a very fast interconversion of the internal aldimine in a highly fluorescent L-serine external aldimine that decays, via the α-carbon proton removal and β-hydroxyl group release, to the α-aminoacrylate Schiff base. This reaction is influenced by protons, monovalent cations, and α-subunit ligands that modulate the distribution between open and closed conformations. In order to identify the ionizable residues that might assist catalysis, we have investigated the pH dependence of the rate of the external aldimine decay by rapid scanning UV-visible absorption and single wavelength fluorescence stopped flow. In the pH range 6–9, the reaction was found to be biphasic with the first phase (rate constants k_1) accounting for more than 70% of the signal change. In the absence of monovalent cations or in the presence of sodium and potassium ions, the pH dependence of k_1 exhibits a bell shaped profile characterized by a pK_{a1} of about 6 and a pK_{a2} of about 9, whereas in the presence of cesium ions, the pH dependence exhibits a saturation profile characterized by a single pK_a of 9. The presence of the allosteric effector indole acetylglycine increases the rate of reaction without altering the pH profile and pK_a values. By combining structural information for the internal aldimine, the external aldimine, and the α-aminoacrylate with kinetic data on the wild type enzyme and β-active site mutants, we have tentatively assigned pK_{a1} to βAsp-305 and pK_{a2} to βLys-87. The loss of pK_{a1} in the presence of cesium ions might be due to a shift to lower values, caused by the selective stabilization of a closed form of the β-subunit.

Structural, dynamic, functional, and regulatory properties of the pyridoxal 5′-phosphate (PLP)[1]-dependent tryptophan synthase (TS) have been thoroughly investigated for more than 4 decades (1–6). The enzyme has been serving as the prototype of allosteric regulation, achieved via ligand-linked stabilization of alternative open-closed tertiary structures of the α- and β-active sites (7–14). Open conformations are endowed with low activity, and closed conformations are endowed with high activity. Tryptophan synthase is a bienzyme that catalyzes the last two steps of L-tryptophan biosynthesis. It is a tetrameric molecule composed of two α- and two β-subunits, forming a linear αββα complex (15). The β-subunit contains a pyridoxal 5′-phosphate molecule bound via a Schiff base to βLys-87. The overall reaction is shown in Reaction 1,

indole-3-glycerolphosphate + L-serine
→ L-tryptophan + D-glyceraldehyde-3-phosphate + H_2O

REACTION 1

Two distinct reactions take place in the α- and β-active sites that are physically separated but connected by an intramolecular channel (15) as shown in Reactions 2 and 3,

α site indole 3-glycerolphosphate
→ indole + D-glyceraldehyde 3-phosphate

REACTION 2

β site indole + L-serine → L-tryptophan + H_2O

REACTION 3

The α-reaction is a concerted catalytic event involving residues Glu-49 and Asp-60, as determined by kinetic and structural studies carried out on the wild type enzyme as well as on several mutants (2). The β-reaction is a more complex process (Scheme 1), requiring the combined action of PLP and several catalytic residues. The mechanism has been inferred by exploiting the distinct spectral properties of transiently accumulating PLP intermediates (1). The internal aldimine absorbs at 412 nm with a minor band at 340 nm. These bands have been attributed to the ketoenamine and enolimine tautomers, respectively (16). The substrate L-serine binds forming a *gem*-diamine complex, characterized by an absorption spectrum centered at 320–330 nm that rapidly converts to a metastable external aldimine. This species absorbs at 420 nm and is the only significantly fluorescent catalytic intermediate (17–21). The removal of the α-proton leads to the formation of a quinonoid species absorbing around 460 nm. This intermediate is particularly labile, and the experimental evidence of its formation is indirect (22). The release of the hydroxyl moiety on the β-carbon completes the first catalytic stage, *i.e.* the β-elimination reaction, with the formation of the α-aminoacrylate. This key catalytic intermediate predominantly absorbs at 350–360 nm extending with broad bands at 470 nm. These bands have been attributed to either the enolimine and ketoenamine tau-

* This work was supported by Grant COFIN2003 (to A. M.) from the Italian Ministry of Instruction, University and Research. This is Paper I in the series "pH Dependence of Tryptophan Synthase Catalytic Mechanism." The costs of publication of this article were defrayed in part by the payment of page charges. This article must therefore be hereby marked "*advertisement*" in accordance with 18 U.S.C. Section 1734 solely to indicate this fact.

** To whom correspondence should be addressed: Dept. of Biochemistry and Molecular Biology, University of Parma, Parco Area delle Scienze 23/A, 43100 Parma, Italy. Tel.: 39-0521-905138; Fax: 39-0521-905151; E-mail: biochim@unipr.it.

[1] The abbreviations used are: PLP, pyridoxal 5′-phosphate; TS, tryptophan synthase; IAG, indole acetylglycine; Bistris propane, 1,3-bis-[tris(hydroxymethyl)methylamino]-propane; Bicine, *N,N*-bis(2-hydroxyethyl)-glycine.

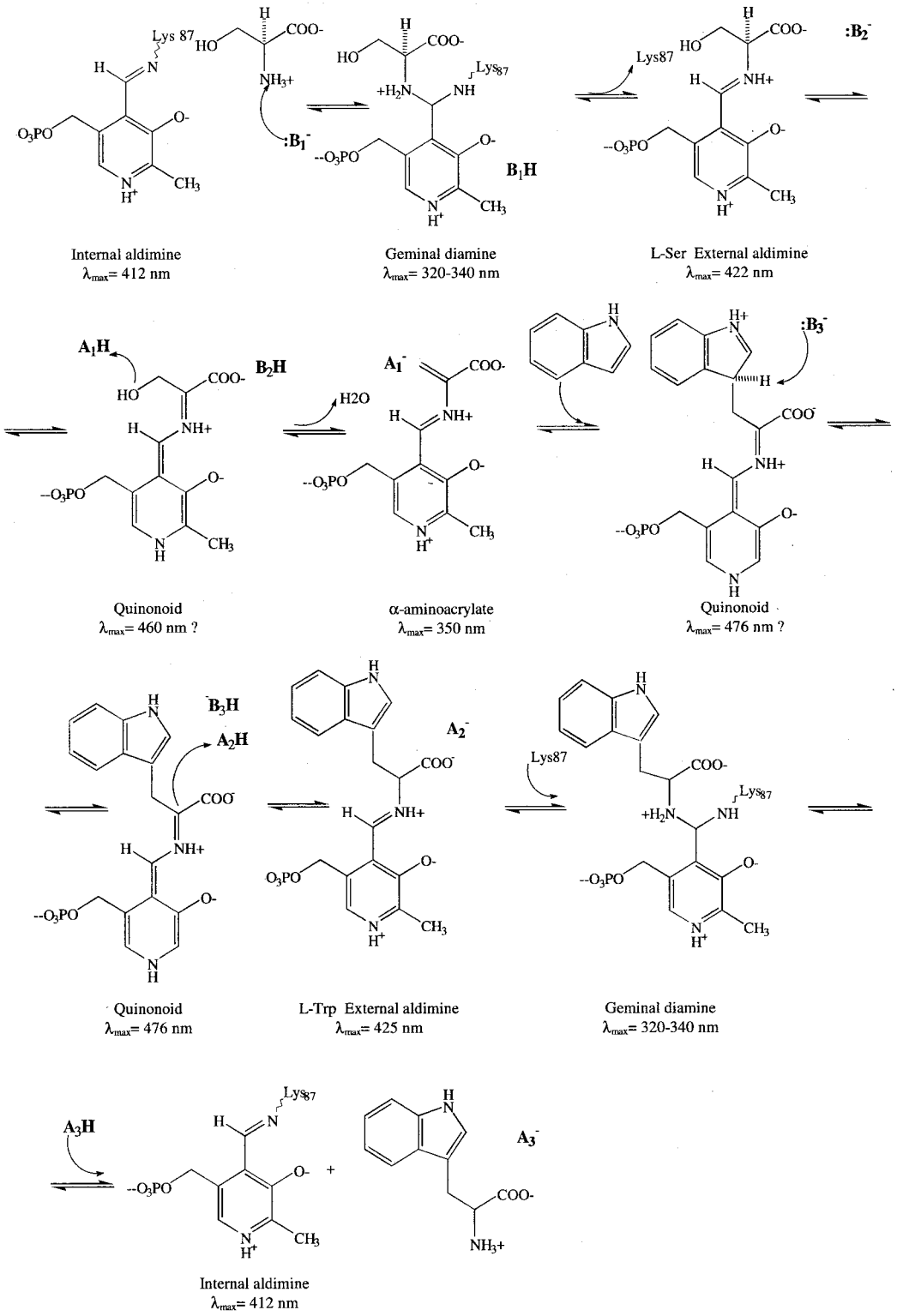

SCHEME 1. **Mechanism of the reaction catalyzed by the β-subunit of tryptophan synthase.**

tomers, respectively (23), or to an unprotonated and protonated aminoacrylate Schiff base, respectively (24). In tyrosine phenol-lyase and tryptophan indole-lyase, the predominant form of the α-aminoacrylate absorbs at 350 nm (25), whereas in *O*-acetylserine sulfhydrylase, the predominant form absorbs at 470 nm (26). In the second stage of the catalytic reaction, indole, channeled from the α-active site, reacts with the α-aminoacrylate double bond forming a quinonoid species that absorbs at about 470 nm. By accepting a proton, the quinonoid species interconverts to the external aldimine of L-tryptophan, absorbing at about 425 nm and devoid of fluorescent properties (27). The release of L-tryptophan completes the catalytic cycle regenerating the internal aldimine.

Several catalytic properties of TS were found to be influenced by pH as follows. (i) The accumulation of the quinonoid species formed in the second stage of the β-reaction increases with pH (28, 29). (ii) The rate-limiting step of the catalytic reaction, carried out by *Escherichia coli* enzyme, varies as a function of

pH, being the Cα proton removal at pH 6.5 and L-tryptophan release at pH 7.6 (18, 30). (iii) The steady-state parameters of *Salmonella typhimurium* wild type TS are pH-dependent, indicating the presence of at least three ionizable residues with pK_{a1} = 6.5, pK_{a2} = 7.25, and pK_{a3} = 8.2–9 (31). (iv) The pH dependence of β-replacement and β-elimination activity was found to be significantly altered in the βHis-86 → Leu mutant (32). (v) The external aldimine accumulation is favored at high pH both in solution and in the crystalline state, whereas the α-aminoacrylate is stabilized at low pH (32–34). (vi) The conversion of the external aldimine to the aminoacrylate is accompanied by the release of a proton originating from the Schiff base nitrogen (24). Surprisingly, no studies have addressed the pH dependence of the catalytic rates on the *S. typhimurium* enzyme, the form for which the three-dimensional structure of the internal aldimine (12, 15, 35), the external aldimine (35, 36), and the α-aminoacrylate (12) has been determined. Recently, it was also found that monovalent cations and α-subunit ligands affect the distribution of intermediates as well as the catalytic properties of TS, triggering regulatory signals and stabilizing alternative open and closed conformations of the α- and β-subunits (23, 27, 37–41). We have investigated the pH dependence of the catalytic rates in the absence and presence of monovalent cations and indole acetylglycine (IAG), a recently discovered α-subunit ligand (13, 42). Here we describe our results on the first stage of the catalytic reaction, the β-elimination, using both rapid scanning UV-visible spectroscopy and single wavelength fluorescence stopped-flow methods. The second stage, the β-addition that completes the β-replacement reaction catalyzed by TS, will be described in a subsequent paper.

MATERIALS AND METHODS

Chemicals and Buffers—Bistris propane, Bicine, L-serine, sodium chloride, potassium chloride, cesium chloride, and IAG were purchased from Sigma. Reagents were of the highest quality commercially available and were used without further purification. Experiments were carried out in solutions containing 25 mM Bistris propane, a metal-free buffer. pH measurements were carried out with a Radiometer pHM83 pH meter, equipped with an Ingold-Mettler LoT406-M3 microelectrode, calibrated with three standard buffers. To obtain the desired pH, HCl was added to solutions.

Enzyme Preparation—The tryptophan synthase $\alpha_2\beta_2$ complex from *S. typhimurium* was purified as described previously (43). The enzyme was stored in 50 mM Bicine buffer, 20 μM PLP, pH 7.8, at −80 °C. Prior to use, the enzyme was extensively dialyzed against 25 mM Bistris propane, pH 7.8.

Kinetic Measurements—Single wavelength kinetic experiments were carried out with a temperature-controlled stopped-flow apparatus, manufactured by Applied Photophysics, using a 75-watt xenon lamp as a light source and a photomultiplier as a detector. The instrumental dead time was 1.5 ms. Rapid spectral scanning stopped-flow measurements were carried out with the same apparatus, using a 150-watt xenon lamp, coupled to a MS 125™ 1/8-m spectrograph and an Instaspec II photodiode array, manufactured by Lot-Oriel. One syringe contained 2.5 mg/ml TS in 25 mM Bistris propane, in the absence and presence of either 250 mM NaCl, 100 mM KCl, or 100 mM CsCl, at the appropriate pH. The second syringe contained 25 mM Bistris propane, 100 mM L-serine, and either no salt or an equal concentration of salt, with or without 2 mM IAG, at the same pH of the first syringe. The pH of the mixed solution was always determined at the end of the experiment. Control experiments carried out with monovalent cations in only one syringe showed the same rate constants and amplitudes. Experiments were carried out over the pH range 6–9 and at 20 °C to ensure enzyme stability. The formation and decay of the external aldimine of L-serine were followed by monitoring fluorescence emission, upon excitation at 420 nm. Kinetic traces at single wavelength were recorded by collecting 1000 data points on a logarithmic scale in 10 s. The photodiode array system collects spectra every 0.0084 s with a 16-μs readout time per pixel. In a typical experiment, background and reference spectra are first collected and stored. In a kinetic series, up to 150 spectra were collected between 335 and 470 nm, in about 1 s.

Data Analysis—Time courses were fitted with Equation 1 describing a biphasic decay,

$$y = y_0 + ae^{-k_1} + be^{-k_2} \quad \text{(Eq. 1)}$$

where y_0 is the floating end point value of the spectroscopic signal; a and b are the amplitudes of the two phases, and k_1 and k_2 are the corresponding rate constants. The pH dependence of the rate constants was fitted with Equations 2 and 3 for two residues or a single ionizable residue (44),

$$k = k_{max}/(1 + 10^{-pH}/10^{-pK_{a1}} + 10^{-pK_{a2}}/10^{-pH} + 10^{-pK_{a2}}/10^{-pK_{a1}}) \quad \text{(Eq. 2)}$$

$$k = k_{max}/(1 + 10^{-pK_{a1}}/10^{-pH}) \quad \text{(Eq. 3)}$$

where k_{max} represents the maximum value of the rate, and pK_{a1} and pK_{a2} are the pK_a values of the ionizable groups. The program Sigma Plot 2000 (SPSS Science) was used to fit the data.

HINT Analysis—The HINT software quantitatively estimates every atom-atom interaction through the equation $b_{ij} = a_i S_i a_j S_j T_{ij} R_{ij} + r_{ij}$, where b_{ij} represents the score value of interacting atoms i and j; a represents the hydrophobic atom constant (45–47), calculated with an adaptation of the fragment constant methods of Abraham and Leo (48); S represents the solvent (water)-accessible surface area; T_{ij} represents a logic function assuming a +1/−1 value depending on the character of interacting polar atoms; R_{ij} represents the exponential function e^{-r}; and r_{ij} represents an implementation of the Lennard-Jones potential. Favorable interactions are positively scored ($b_{ij} > 0$), whereas unfavorable ones are negatively scored ($b_{ij} < 0$). The total score that evaluates the strength of the binding process is $\Sigma_i\Sigma_j b_{ij} = \Sigma_i\Sigma_j(a_i S_i a_j S_j T_{ij} R_{ij} + r_{ij})$. Because each atom-atom interaction (b_{ij}) is related to a partial free energy variation (δg), the total score ($\Sigma_i\Sigma_j b_{ij}$) is automatically correlated to the sum of each δg and, therefore, to global interaction binding free energy ($\Delta G_{interaction}$) (49–52). The entropic contribution given by the release of water to bulk, which follows molecular association, is implicitly incorporated in the hydrophobic atom constants derived from partition measurements (53). The HINT procedure consists of two steps as follows: the model building and the hydrophatic analysis, as described previously (49). Three-dimensional coordinates of TS derivatives were retrieved from Protein Data Bank and imported into Sybyl (version 6.9, www.tripos.com). The structures were properly modeled, checking atom and bond types and adding hydrogen atoms, using Sybyl tools. The automatic algorithms do not account for intermolecular and intramolecular steric clashes; thus hydrogens were energy-minimized by using Powell algorithm with a gradient of 0.5 kcal (mol Å)$^{-1}$ for 1500 cycles. The ionizable groups of interacting residues at the binding site were carefully analyzed, and different possible protonation states were considered and computed. The hydropathic analysis was performed with HINT (version 2.35S, www.tripos.com). $LogP_{o/w}$ was calculated for each interacting component using the "All" option. The "Neutral" option was chosen for the solvent condition when the ionization state of residues was not changed, whereas "inferred" was the option adopted for the partition procedure when the ionization state was modified. The HINT score was finally calculated for each couple of interacting residues at the active site.

RESULTS

The reaction of TS with L-serine at different pH values, in the absence (Fig. 1, *a–c*) and presence of sodium (Fig. 1, *d–f*), potassium (Fig. 1, *g–i*), and cesium ions (Fig. 1, *j–l*), was first monitored by rapid scanning stopped flow to detect simultaneously all forming and decaying catalytic intermediates. Such an informative approach was pioneered by Dunn and co-workers (22, 54). The external aldimine with L-serine, absorbing at 422 nm, is formed in 20–30 ms (Fig. 1, *spectrum 1*, 33 ms) and rapidly decays to accumulate the α-aminoacrylate Schiff base, predominantly absorbing at 350 nm (Fig. 1, *spectrum 5*, ~1 s). The amount of transiently formed external aldimine, as well as the relative amount of external aldimine and α-aminoacrylate Schiff base at the end of the reaction, are strongly dependent on pH and monovalent cations. The same reaction was monitored by single wavelength stopped flow by recording the fluorescence emission of the external aldimine, upon excitation at 420 nm, in the absence (Fig. 2*a*) and presence of 250 mM NaCl (Fig. 2*b*), 100 mM KCl (Fig. 2*c*), and 100 mM CsCl (Fig. 2*d*) at pH values between 6 and 8.8. The kinetics were well fitted to a

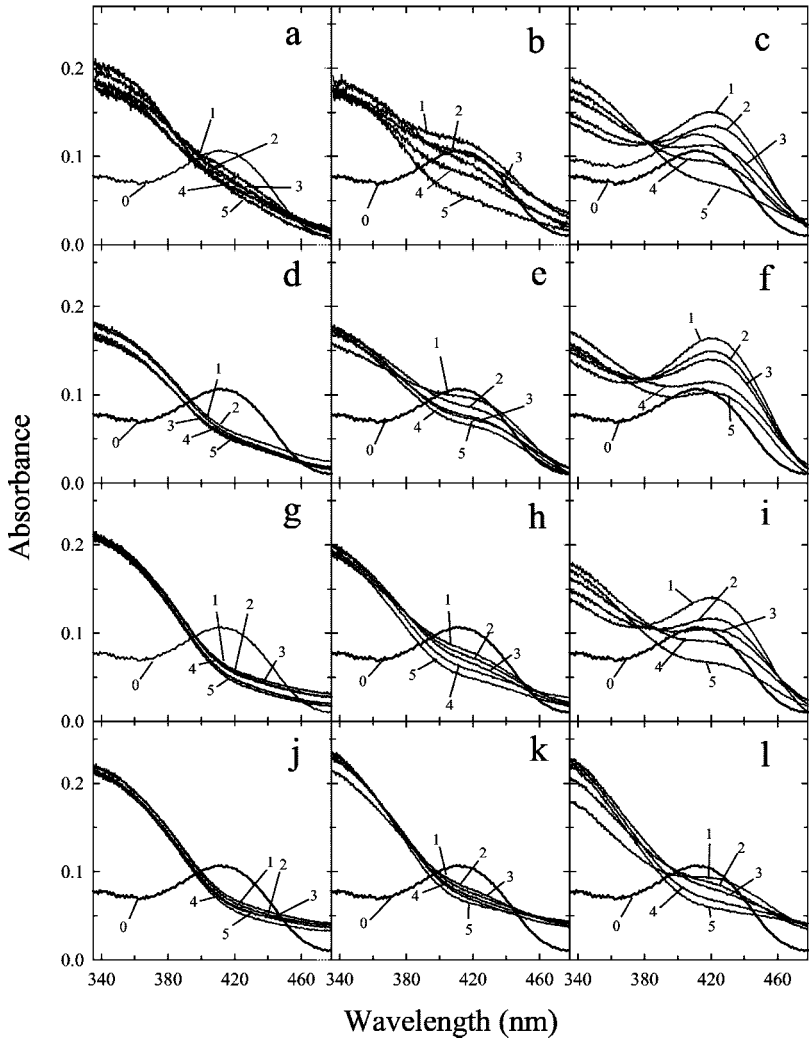

FIG. 1. **Rapid scanning stopped-flow spectra for the reaction of TS with L-serine in the absence of metal ions at pH 6.2 (*a*), 7.8 (*b*), 8.7 (*c*), and in the presence of 250 mM NaCl at pH 6.2 (*d*), 7.8 (*e*), 8.7 (*f*), 100 mM KCl at pH 6.2 (*g*), 7.8 (*h*), 8.7 (*i*), 100 mM CsCl at pH 6.2 (*j*), 7.8 (*k*), and 8.7 (*l*).** The conditions after mixing are as follows: 50 mM L-serine, 10 μM $\alpha_2\beta_2$ TS, 25 mM Bis-Tris propane. The timing sequences are as follows: 0 s (*spectrum 0*), 0.0336 s (*spectrum 1*), 0.084 s (*spectrum 2*), 0.168 s (*spectrum 3*), 0.798 s (*spectrum 4*), and 0.9492 s (*spectrum 5*).

biexponential process (Table I), as reported previously (22, 54). Actually, there is a third very slow phase, characterized by a small amplitude, that we neglected, considering it to be catalytically irrelevant, in agreement with other studies (19, 22, 30). The rate constants determined at pH 7.8 in the absence and presence of sodium or potassium ions are in good agreement with those observed previously (27, 37, 39). The amplitude of the first phase A_1 generally accounted for over 70% of the fluorescence change (Table I) and did not show any pH dependence. In contrast, the corresponding rate k_1 (Table I) exhibited either a bell-shaped profile, as in the absence and presence of potassium and sodium ions (Fig. 3*a*), or a saturating profile, as in the presence of cesium ions (Fig. 3*b*), indicating that the formation of α-aminoacrylate is controlled by either two or only a single ionizable residue, respectively. The pK_a values, determined according to Equations 2 and 3 (see "Materials and Methods"), are reported in Table II. The pK_{a1} exhibits a value ranging from 5.8 or 5.9, in the presence of sodium and potassium ions, respectively, to 6.4 in the absence of monovalent cations. The pK_{a2} exhibits values close to 9 for all experimental conditions. An analysis of the pH profile in the presence of cesium ions by using two pK_a values leads to a pK_{a1} of 5.20 and pK_{a2} of 9.02 with an R^2 of 0.83, a value only slightly higher than that (0.78) obtained with the analysis assuming a single pK_a (Table II). Both the very small improvement of the quality of the fitting and a value of pK_{a1} clearly out of the pH range of experimental data make very questionable the presence of two pK_a values in the presence of cesium ions. The maximal rate of reaction follows the order: $Cs^+ > K^+ >$ no ions $> Na^+$. An analysis based on the pH dependence of log k shows very similar pK_a values and a slope close to unity, indicating that single ionizable residues are responsible for each pK_a (data not shown). Furthermore, the dependence on pH of the rate k_2 exhibits a bell shape only in the presence of sodium ions (Table I).

To investigate the effect of α-subunit ligands on the pH dependence of the α-aminoacrylate formation, the reaction of TS with L-serine was carried out in the presence of the allosteric effector IAG (42, 55), with and without monovalent cations. IAG was preferred to glycerol 3-phosphate because it is commercially available free of ions. Representative time courses at different pH values in the absence (Fig. 4*a*) and presence of sodium (Fig. 4*b*), potassium (Fig. 4*c*), and cesium ions (Fig. 4*d*) are shown. Independently of experimental conditions, the rate of reaction in the presence of IAG was found to be 1.2–1.8-fold higher than in its absence. A 3–4-fold increase of the rate was observed previously for this reaction at pH 7.8 in the presence of α-glycerol 3-phosphate (7, 8). The kinetics was fitted to a biexponential decay with the first phase accounting for most of the amplitude (Table III). The pH dependence of k_1, reported in Fig. 5, exhibits the same profile as observed previously in the absence of IAG. The calculated pK_{a1} and pK_{a2} values (Table IV) are very close to those found in the absence of IAG. Also in this case, an analysis of the pH profile in the presence of cesium ions using two pK_a values leads to a negligible improvement of the quality of the fitting and to an

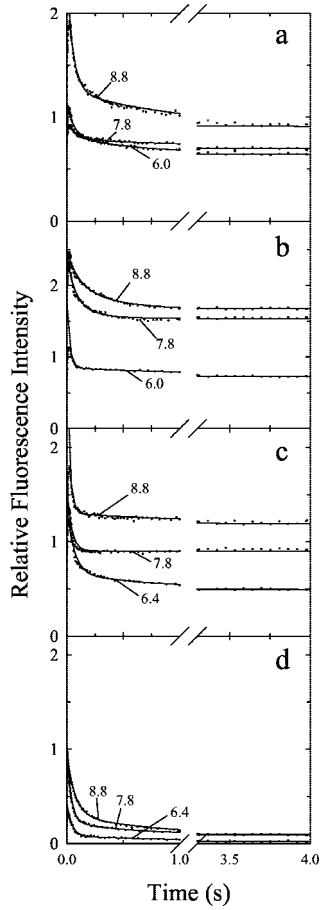

FIG. 2. **Time courses for the reaction of TS with L-serine.** The kinetics was recorded by monitoring the fluorescence intensity upon excitation at 420 nm, in the absence of monovalent ions (*a*), and in the presence of 250 mM NaCl (*b*), 100 mM KCl (*c*), 100 mM CsCl (*d*), at the indicated pH values. The conditions after mixing are as follows: 50 mM L-serine, 10 μM $\alpha_2\beta_2$ TS, 25 mM Bis-Tris propane. The *solid line* through data points represents the fitting to a biexponential decay process.

unreliable value for pK_{a1} (Table IV).

The dependence on the pH of the amount of the external aldimine, as determined from the emission intensity after 10 s of reaction (condition of quasi-equilibrium) in the presence of sodium ions (Fig. 6), was found to closely match the equilibrium distribution of the external aldimine and α-aminoacrylate determined previously (33, 34). High pH stabilizes the external aldimine, and low pH stabilizes the α-aminoacrylate. In the presence of potassium ions, in the absence of monovalent cations, and in the presence of cesium ions the amount of external aldimine at quasi-equilibrium becomes progressively lower, exhibiting a weaker dependence on pH. This behavior is even more marked when IAG is bound to the α-subunits (data not shown).

DISCUSSION

In the first stage of the reaction catalyzed by TS, there are at least three steps that may require the presence of a proton donor/acceptor residue (Scheme 1). The same holds for the second stage. B_1 deprotonates the incoming α-amine of L-serine to obtain a nucleophilic group that attacks the carbon of the Schiff base to form the *gem*-diamine. This deprotonation might not be required at physiological pH because the pK_a of the α-amine for a free amino acid is close to 8.3. B_2 removes the α-proton of L-serine external aldimine to generate a quinonoid species. A_1H donates a proton to the β-hydroxyl group to facilitate its release as a water molecule, with the concomitant formation of the α-aminoacrylate Schiff base. In the second half of the reaction, upon indole attack to the α-aminoacrylate species, B_3 accepts a proton from the indolenine derivative; A_2H donates a proton to the α-carbon of the quinonoid species to form the external aldimine of L-tryptophan, and finally, A_3H donates a proton to the amine of L-tryptophan to release it as a zwitterion. It is obvious that basic residues that accept a proton

TABLE I
Rate constants and amplitude for the decay of the external aldimine species as a function of pH, in the absence and presence of 250 mM NaCl, 100 mM KCl, and 100 mM CsCl

Values are the average of at least five time courses.

pH	k_1	k_2	A_1
	s^{-1}		%
	No metal ion		
6.05	5.65 ± 0.75	0.73 ± 0.35	57 ± 8
6.27	7.62 ± 0.40	0.91 ± 0.10	74 ± 3
6.46	10.64 ± 0.48	1.24 ± 0.15	84 ± 2
6.68	12.56 ± 0.56	0.82 ± 0.10	79 ± 4
6.90	13.70 ± 0.57	0.69 ± 0.06	74 ± 2
7.07	16.14 ± 0.46	0.77 ± 0.19	95 ± 1
7.24	16.23 ± 0.42	0.81 ± 0.16	90 ± 1
7.46	16.95 ± 0.43	0.78 ± 0.19	94 ± 1
7.63	16.00 ± 0.39	0.97 ± 0.13	87 ± 1
7.87	15.80 ± 0.48	0.62 ± 0.09	85 ± 1
8.06	15.70 ± 0.47	0.65 ± 0.13	90 ± 1
8.25	14.90 ± 0.44	0.64 ± 0.13	90 ± 1
8.47	13.65 ± 0.48	0.54 ± 0.11	80 ± 1
8.73	11.20 ± 0.50	0.55 ± 0.04	79 ± 1
	NaCl		
6.05	11.33 ± 0.30	0.90 ± 0.02	56 ± 1
6.27	12.48 ± 0.27	0.89 ± 0.02	64 ± 1
6.46	12.86 ± 0.24	1.01 ± 0.03	67 ± 1
6.68	13.95 ± 0.30	1.13 ± 0.05	77 ± 1
6.90	14.58 ± 0.32	1.38 ± 0.09	77 ± 1
7.07	15.62 ± 0.39	1.57 ± 0.13	84 ± 1
7.24	15.99 ± 0.42	1.47 ± 0.18	84 ± 1
7.46	16.19 ± 0.46	1.56 ± 0.16	84 ± 1
7.63	15.24 ± 0.49	2.27 ± 0.19	81 ± 2
7.87	15.67 ± 0.62	2.48 ± 0.18	75 ± 2
8.06	15.53 ± 0.64	2.48 ± 0.21	75 ± 2
8.30	14.26 ± 0.69	3.10 ± 0.82	74 ± 1
8.60	11.53 ± 0.22	1.07 ± 0.02	67 ± 2
8.73	12.24 ± 1.52	1.12 ± 0.02	66 ± 1
	KCl		
6.05	11.97 ± 0.53	1.08 ± 0.08	69 ± 2
6.27	14.30 ± 0.26	0.12 ± 0.05	72 ± 1
6.46	16.71 ± 0.23	1.25 ± 0.07	82 ± 1
6.68	17.70 ± 0.17	1.02 ± 0.06	87 ± 1
6.90	18.04 ± 0.22	0.88 ± 0.08	90 ± 1
7.24	19.72 ± 0.31	0.74 ± 0.20	72 ± 1
7.46	20.37 ± 0.31	0.62 ± 0.12	92 ± 1
7.63	19.97 ± 0.32	1.15 ± 0.15	89 ± 1
7.87	18.49 ± 0.41	0.63 ± 0.15	96 ± 1
8.06	17.04 ± 0.20	0.83 ± 0.07	89 ± 1
8.25	14.91 ± 0.28	1.72 ± 0.24	91 ± 1
8.47	13.45 ± 0.29	1.34 ± 0.16	89 ± 1
8.65	11.64 ± 0.79	1.78 ± 0.24	88 ± 1
8.73	11.66 ± 0.69	0.54 ± 0.18	62 ± 1
	CsCl		
6.19	24.51 ± 0.30	0.58 ± 0.03	87 ± 1
6.20	23.51 ± 0.33	0.56 ± 0.12	93 ± 1
6.40	22.54 ± 0.32	0.75 ± 0.07	92 ± 1
6.46	22.71 ± 0.29	0.93 ± 0.05	83 ± 1
6.73	24.22 ± 0.95	0.60 ± 0.03	87 ± 1
7.02	23.29 ± 0.20	1.23 ± 0.05	85 ± 1
7.05	24.42 ± 0.42	1.66 ± 0.08	80 ± 1
7.22	25.63 ± 0.48	1.45 ± 0.20	90 ± 1
7.60	25.66 ± 0.21	0.96 ± 0.03	83 ± 1
7.80	25.17 ± 0.24	1.19 ± 0.12	97 ± 1
8.06	22.32 ± 0.28	1.08 ± 0.17	71 ± 1
8.45	21.00 ± 0.15	0.92 ± 0.04	89 ± 1
8.65	18.59 ± 0.64	1.35 ± 0.04	74 ± 1
8.70	15.30 ± 0.28	1.34 ± 0.05	70 ± 1

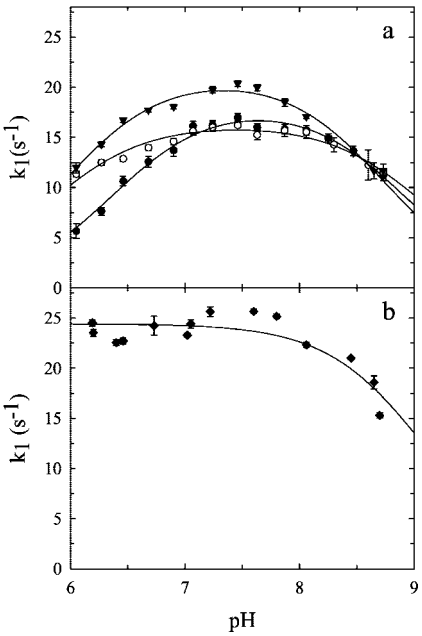

FIG. 3. **pH dependence of the first rate constant, k_1, calculated from the fluorescence intensity decay of the external aldimine of L-serine, (*a*) in the absence of metal ions (*closed circles*), in the presence of 250 mM NaCl (*open circles*), 100 mM KCl (*closed inverted triangles*), and (*b*) 100 mM CsCl (*closed diamonds*).** The *solid lines* represent the regression curve to either Equation 2 or 3.

TABLE II
pK_a values calculated from the pH dependence of the first rate constant of external aldimine decay (k_1), in the absence and presence of 250 mM NaCl, 100 mM KCl, 100 mM CsCl

Equation 2 was used to fit the data in the absence and presence of NaCl and KCl, and either Equation 2 or 3 was used for data in the presence of CsCl.

Metal ion	pK_{a1}	pK_{a2}	R^2
	6.37 ± 0.04	8.91 ± 0.05	0.98
Na^+	5.78 ± 0.05	9.11 ± 0.06	0.93
K^+	5.94 ± 0.05	8.73 ± 0.04	0.97
Cs^+	5.20 ± 0.23	9.02 ± 0.08	0.83
Cs^+		9.10 ± 0.08	0.78

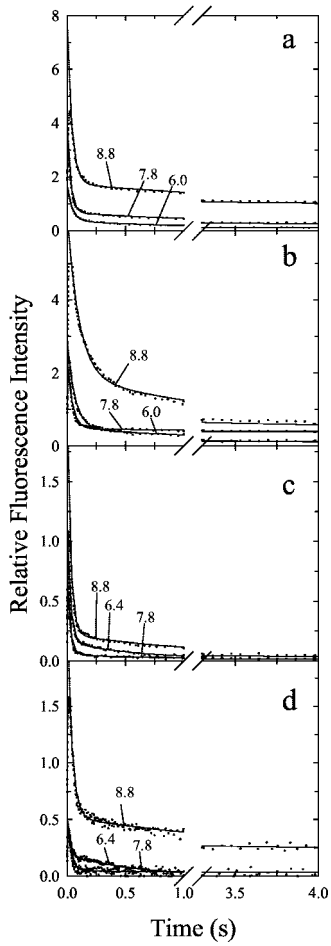

FIG. 4. **Time courses for the reaction of TS with L-serine, in the presence of IAG.** The kinetics was recorded by monitoring the fluorescence intensity upon excitation at 420 nm, in the absence of monovalent cations (*a*), and in the presence of 250 mM NaCl (*b*), 100 mM KCl (*c*), and 100 mM CsCl (*d*) at the indicated pH values. The conditions after mixing are as follows: 50 mM L-serine, 10 μM $\alpha_2\beta_2$ TS, 1 mM IAG, 25 mM Bis-Tris propane. The *solid lines* through data points represent the fitting to a biexponential decay.

may coincide with acidic residues donating a proton in a later step and vice versa. In the present work, we addressed the following: (i) whether the pH dependence of the catalytic rates is consistent with Scheme 1; (ii) whether the open-closed conformational equilibrium affects the pH dependence; and (iii) whether it is possible to identify the ionizable residues that are responsible for the observed pH dependence. It is important to point out that we have measured time courses directly related to the interconversion of enzyme-substrate complexes, and therefore, the corresponding pH profiles of the rate constants reflect ionization properties of the enzyme-substrate complexes (56).

The first part of the time course of the reaction between TS and L-serine, monitored by absorbance at 420 nm and fluorescence emission upon excitation at the same wavelength, indicates a very fast formation of the external aldimine that is completed in 20–30 ms. In this part of the kinetics, the relatively noisy data preclude a detailed analysis of the pH dependence. Therefore, we do not have information on the residue that might deprotonate L-serine, and we cannot determine whether this first deprotonation event takes place. The second part of the time course is a fluorescence decrease, associated with the disappearance of the external aldimine with the concomitant accumulation of the α-aminoacrylate. This step is strongly pH-dependent and is affected by the presence of monovalent cations and α-subunit ligands (Figs. 4 and 6). The rate constants, determined at pH 7.8, are in good agreement with previous studies carried out at the same pH (27, 37, 39, 57), showing that the decay of the external aldimine is slower in the presence of sodium ions with respect to a monovalent cation-free solution and is faster in the presence of potassium and cesium ions (Table I). On the basis of data collected at pH 7.8, it was proposed that in the absence of monovalent cations both the external aldimine and the α-aminoacrylate form are in the less active open conformation; in the presence of sodium ions the external aldimine is in a partially open conformation and the aminoacrylate is in a closed conformation, and in the presence of cesium ions the aminoacrylate is in the more active closed state (23, 27, 37, 39). However, within a defined conformation cations are clearly able to modulate differently the reactivity of the β-subunit and its pH dependence. Unfortunately, the structural basis of this fine effect cannot be fully understood because no three-dimensional structure of TS free of ions is available either in the absence or presence of L-serine. By phosphorescence spectroscopy, it was observed that the compactness of the enzyme increases in the presence of monovalent ions (23). Finally, on the basis of the comparison of the pH profile in the absence and presence of monovalent ions, it seems that the role

TABLE III

Rate constants and amplitude for the decay of the external aldimine as a function of pH, in the presence of 1 mM IAG, in the absence and presence of 250 mM NaCl, 100 mM KCl, 100 mM CsCl

Values are the average of at least five time courses.

pH	k_1	k_2	A_1
	s^{-1}		%
	No metal ions + IAG		
6.15	20.47 ± 1.80	1.53 ± 0.24	74 ± 3
6.31	21.87 ± 0.38	1.59 ± 0.12	83 ± 1
6.52	25.62 ± 0.98	1.53 ± 0.15	81 ± 2
6.80	30.00 ± 0.58	2.37 ± 0.10	77 ± 1
6.95	31.06 ± 0.56	1.26 ± 0.10	85 ± 1
7.24	32.42 ± 0.43	1.00 ± 0.03	79 ± 1
7.30	31.84 ± 0.23	1.06 ± 0.04	88 ± 1
7.50	34.33 ± 0.31	0.67 ± 0.07	92 ± 1
7.71	32.92 ± 0.34	0.68 ± 0.04	87 ± 1
7.80	33.40 ± 0.36	0.87 ± 0.06	89 ± 1
8.20	29.00 ± 0.25	0.37 ± 0.03	87 ± 1
8.47	23.99 ± 0.31	0.15 ± 0.02	85 ± 1
8.56	23.10 ± 0.35	0.37 ± 0.04	87 ± 1
8.63	22.00 ± 0.15	0.12 ± 0.01	57 ± 2
9.00	12.75 ± 0.37	0.22 ± 0.06	80 ± 1
	NaCl + IAG		
6.05	15.32 ± 0.13	0.62 ± 0.03	85 ± 1
6.31	17.32 ± 0.21	0.53 ± 0.06	89 ± 1
6.47	19.95 ± 0.21	0.50 ± 0.04	88 ± 1
6.80	20.51 ± 0.20	0.41 ± 0.07	93 ± 1
7.05	23.84 ± 0.32	0.73 ± 0.03	79 ± 1
7.24	23.28 ± 0.35	0.96 ± 0.10	89 ± 1
7.30	24.79 ± 0.34	0.62 ± 0.14	95 ± 1
7.71	22.97 ± 0.38	0.45 ± 0.12	89 ± 1
7.77	22.93 ± 0.29	0.41 ± 0.12	96 ± 1
7.80	22.09 ± 0.34	0.71 ± 0.10	91 ± 1
8.06	20.15 ± 0.29	0.47 ± 0.08	93 ± 1
8.20	19.52 ± 0.29	0.34 ± 0.07	93 ± 1
8.58	19.39 ± 0.34	0.28 ± 0.06	89 ± 1
8.71	16.28 ± 0.33	0.33 ± 0.04	81 ± 1
8.78	14.56 ± 0.25	0.43 ± 0.06	84 ± 1
9.00	9.90 ± 0.17	0.59 ± 0.17	75 ± 1
	KCl + IAG		
6.13	27.55 ± 0.57	0.88 ± 0.05	86 ± 1
6.31	30.00 ± 0.34	1.34 ± 0.25	85 ± 1
6.40	32.42 ± 0.30	0.99 ± 0.04	95 ± 1
6.61	33.68 ± 0.30	0.74 ± 0.10	90 ± 1
6.80	34.94 ± 0.27	1.81 ± 0.05	86 ± 1
6.90	34.55 ± 0.34	0.12 ± 0.03	90 ± 1
7.24	37.61 ± 0.43	1.05 ± 0.06	89 ± 1
7.50	36.71 ± 0.29	1.53 ± 0.16	93 ± 1
7.95	36.32 ± 0.25	0.69 ± 0.05	95 ± 1
8.20	32.06 ± 0.25	0.70 ± 0.02	93 ± 1
8.47	28.54 ± 0.23	0.70 ± 0.02	88 ± 1
8.56	24.67 ± 0.30	0.65 ± 0.03	81 ± 1
8.68	24.15 ± 0.54	0.70 ± 0.10	83 ± 1
9.00	22.00 ± 0.34	0.46 ± 0.05	88 ± 1
	CsCl + IAG		
6.17	33.36 ± 3.44	2.37 ± 0.28	72 ± 1
6.28	32.28 ± 3.24	1.36 ± 0.18	72 ± 2
6.40	33.46 ± 0.79	2.18 ± 0.15	67 ± 1
6.85	33.77 ± 0.91	1.42 ± 0.05	76 ± 1
7.30	33.54 ± 1.17	1.50 ± 0.21	86 ± 1
7.60	32.09 ± 0.68	0.80 ± 0.08	90 ± 1
7.71	32.09 ± 0.35	0.83 ± 0.02	80 ± 2
7.88	33.01 ± 0.89	1.81 ± 0.18	85 ± 1
8.10	32.80 ± 0.54	0.65 ± 0.09	92 ± 1
8.47	29.88 ± 0.60	0.22 ± 0.04	85 ± 1
8.56	23.62 ± 0.91	0.63 ± 0.03	83 ± 1
8.63	23.00 ± 0.32	0.46 ± 0.08	92 ± 2
9.00	19.05 ± 0.35	0.46 ± 0.05	84 ± 1

of cations is essentially conserved over the entire pH range we have explored.

The more striking difference in the effect of monovalent cations on the pH dependence of the catalytic rate is the change in pH profile, bell-shaped both in the absence and presence of sodium and potassium ions and pH-independent below 8.0 in the presence of cesium ions. This behavior indicates that, in the absence and presence of sodium and potassium ions, two ionizable residues are responsible for the pH dependence of the catalytic rate in the disappearance of the external aldimine and

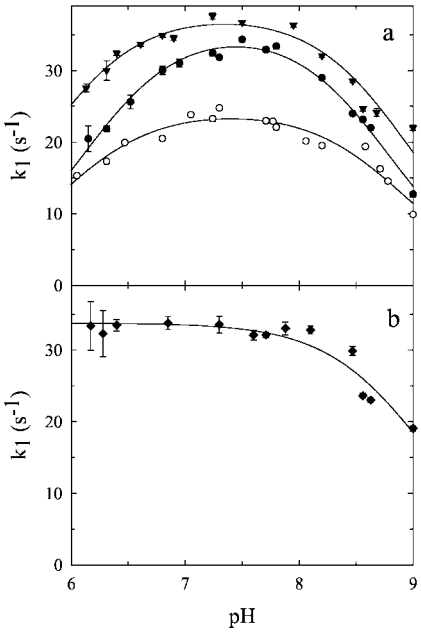

FIG. 5. **pH dependence of the first rate constant, k_1, calculated from the fluorescence intensity decay of the external aldimine of L-serine with 1 mM IAG, (*a*) in the absence of metal ions (*closed circles*), in the presence of 250 mM NaCl (*open circles*), 100 mM KCl (*closed inverted triangles*), and (*b*) 100 mM CsCl (*closed diamonds*).** The *solid lines* represent the regression curve to either Equation 2 or 3.

TABLE IV

pK_a values calculated from the pH dependence of the first rate constant of external aldimine decay (k_1), in the presence of 1 mM IAG, and in the absence and presence of 250 mM NaCl, 100 mM KCl, 100 mM CsCl

Equation 2 was used to fit the data in the absence and presence of NaCl and KCl, and either Equation 2 or 3 was used for data in the presence of CsCl.

Metal ion	Ligand	pK_{a1}	pK_{a2}	R^2
	IAG	6.10 ± 0.03	8.79 ± 0.03	0.98
Na^+	IAG	5.87 ± 0.08	8.94 ± 0.06	0.92
K^+	IAG	5.71 ± 0.09	9.98 ± 0.06	0.91
Cs^+	IAG	4.85 ± 0.44	9.05 ± 0.06	0.92
Cs^+	IAG		9.08 ± 0.06	0.91

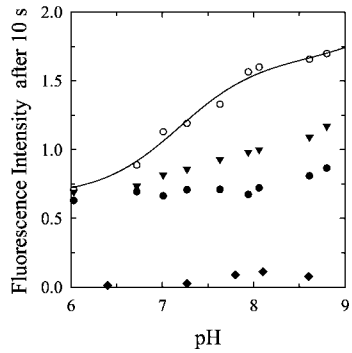

FIG. 6. **pH dependence of the relative fluorescence intensity collected after 10 s of the reaction between TS and 50 mM L-serine, in the absence of metal ions (*closed circles*), and in the presence of 250 mM NaCl (*open circles*), 100 mM KCl (*closed inverted triangles*), 100 mM CsCl (*closed diamonds*).** The *solid line* through data points represents the fitting to Equation 2.

accumulation of α-aminoacrylate, whereas only a single ionizable residue controls the reaction rate in the presence of cesium ions, at least in the pH range 6–9. Under all experimental conditions, pK_{a1} is close to 6, and pK_{a2} is close to 9 (Table II). The absence of pK_{a1} when cesium ions are bound to the enzyme can have two distinct explanations. The first explanation is that pK_{a1} is shifted to lower values and cannot be observed because of the limited enzyme stability below pH 6. The second explanation is that in the closed conformation the ionizable residue responsible for pK_{a1} is no more relevant in the transformation of the external aldimine than into the α-aminoacrylate. It is interesting to note that the same pattern with similar pK_a values holds when IAG, an allosteric effector bound to the α-subunit, is present both in the absence and presence of ions (Table IV). All rates are higher in the presence of IAG in keeping with the role of the allosteric effectors to stabilize the closed conformation in the presence of monovalent cations (27, 37, 39). On the basis of these data it seems more plausible that pK_{a1} is shifted to lower values due to specific effects of cesium ions on the ionizable residue either via direct or indirect interactions. It should be made clear that a single pK_a does not necessarily correspond to an individual group because pK_a is a group function (58). The pK_{a1} and pK_{a2} values closely correspond to the pK_{a1} and pK_{a3} values determined by investigating the pH dependence of the steady-state parameters (31). On the other hand, we do not observe the intermediate pK_{a2} of 7.25 that these authors detected. This finding is not surprising because we have presently investigated the first stage of the reaction, whereas steady-state parameters reflect the overall β-replacement reaction. Indeed, we have observed a pK_a of about 7.5 that controls the rate of formation of the quinonoid species that originates in the reaction between indole and L-serine in the second stage of TS catalysis.[2]

In order to identify the ionizable residues responsible for the control of the chemical transformation from the external aldimine to α-aminoacrylate, there are two sources of information, the three-dimensional structures of the native enzyme and catalytic intermediates and the kinetic data obtained for the wild type enzyme and mutants. The more relevant available structures are as follows: (i) the internal aldimine in the presence of either sodium (12, 15, 35, 40), potassium, or cesium ions (40), also with bound α-subunit ligands (12, 55); (ii) the external aldimine of the wild type enzyme in the presence of sodium ions (35); and (iii) the α-aminoacrylate Schiff base in the presence of sodium ions and 5-fluoroindole propanol phosphate, an α-subunit ligand (12). Other structures of the internal and external aldimine, determined on mutant enzymes (35, 36, 41, 59, 60), should be considered with caution, because mutation might have small but critical consequences on the location and local environment of ionizable residues. Furthermore, as pointed out earlier, no structure is available in the absence of monovalent cations at any stage of the catalytic cycle.

On the basis of the three-dimensional structures of the internal aldimine (12, 15, 35), the external aldimine (35), and the aminoacrylate (12), there are several ionizable residues within the β-active site that, to some extent, could assist the reaction with an acid-base catalysis: βHis-86, βLys-87, βGlu-109, βHis-115, βLys-167, and βAsp-305 (Fig. 7). However, βHis-86 was proposed to be involved in the interaction with the PLP phosphate group and, possibly, in the lowering of the pK_a of βLys-87 (32). There are also ionizable groups on PLP, but spectral evidence indicates a pH independence for their ionization state during the catalytic cycle (28, 33, 34).

[2] F. Schiaretti, S. Bettati, and A. Mozzarelli, unpublished observations.

βLys-87 is bound to PLP in the internal aldimine (Fig. 7*a*). In the external aldimine, βLys-87 appears to interact with the phosphate moiety of PLP (Fig. 7*b*). The distance between the Nε and the phosphate oxygen atoms varies between 3.22 and 5.26 Å. An evaluation of the strength of this interaction using HINT software (46, 47, 49) indicates that, assuming either a protonated or neutral amine, the HINT score is about 2000 and 400, respectively. It was found that about 500 HINT score units correspond to a binding free energy of 1 kcal/mol (49). From structural data it is not possible to determine whether the Nε group is protonated because x-ray data at 2.3 Å resolution cannot reveal hydrogen atoms. It was proposed (35) that a rotation of βLys-87 side chain would take the amine group at 2.8 Å from the Cα atom of serine external aldimine, a favorable distance for a neutral amine to extract a proton. However, careful inspection suggests that βLys-87 side chain is not free to move because the amine is taken in check by the carbonyl group of βGly-189. In the α-aminoacrylate structure (Fig. 7*c*), βLys-87 occupies almost the same position as in the external aldimine with a distance of the Nε to phosphate oxygen of 3.64–5.60 Å and an interaction strength of 1500 and 300 HINT score units, assuming a protonated and neutral amine, respectively. This finding is somewhat surprising if, as generally assumed, βLys-87 is the residue that extracts the serine Cα proton. Protonation of βLys-87 should lead to a structural reorganization of the surrounding groups. A possibility might be that βLys-87 abstracts the proton and donates it to the β-hydroxyl of L-serine or to some other basic residue. βLys-87 was proposed previously to act as the base that abstracts the α-carbon proton on the basis of kinetic (61, 62) and structural studies on the mutant βLys-87 → Thr (36). The reaction between L-serine and the mutant βLys-87 → Thr proceeds only to the formation of the external aldimine. However, the presence of ammonium chloride allows us to recover the activity, thus suggesting that a base is required for the removal of the α-carbon proton (61). Furthermore, βLys-87 seems to assist the transaldimination and product release to favor the β-hydroxyl removal and to donate a proton to the quinonoid of L-tryptophan (62). The latter role should imply that the ε-amine is neutral at the stage of the external aldimine and protonated at the stage of the α-aminoacrylate intermediate. It was also found that in the mutant βLys-87 → Thr the substrate analog β-chloroalanine is slowly converted to the α-aminoacrylate (62), likely because it possesses a good leaving group and does not require assistance by the enzyme catalytic machinery.

In the internal aldimine βGlu-109 is located at about 11 Å from C-4′ of PLP and does not interact with any PLP atoms (Fig. 7*a*). The distance of the carboxylate oxygens from the nitrogen atoms of βHis-115 imidazole ring is 4.35–6.00 Å, suggesting a weak interaction. This distance remains almost the same in the external aldimine (Fig. 7*b*) and in the aminoacrylate species (Fig. 7*c*). The carboxylate oxygens of βGlu-109 are also at about 6.5 Å from the carboxylate oxygens of L-serine, weakly anchoring the substrate in the active site. Furthermore, the distance between the carboxylate oxygens and the β-hydroxyl group is about 8.5 Å, making it very unlikely that βGlu-109 plays a catalytic role assisting in β-hydroxyl elimination (63). βGlu-109 was proposed to activate the incoming indole to facilitate its reaction with aminoacrylate (36, 64). The pH dependence of the catalytic rates of the first stage does not exhibit a pK_a of 7.25, detected instead in the overall β-reaction (31). This finding clearly indicates that this pK_a pertains to an ionizable residue that is relevant in the second stage of the reaction.

βHis-115 is located in the active site with the imidazole ring pointing away from the PLP both in the internal aldimine (Fig.

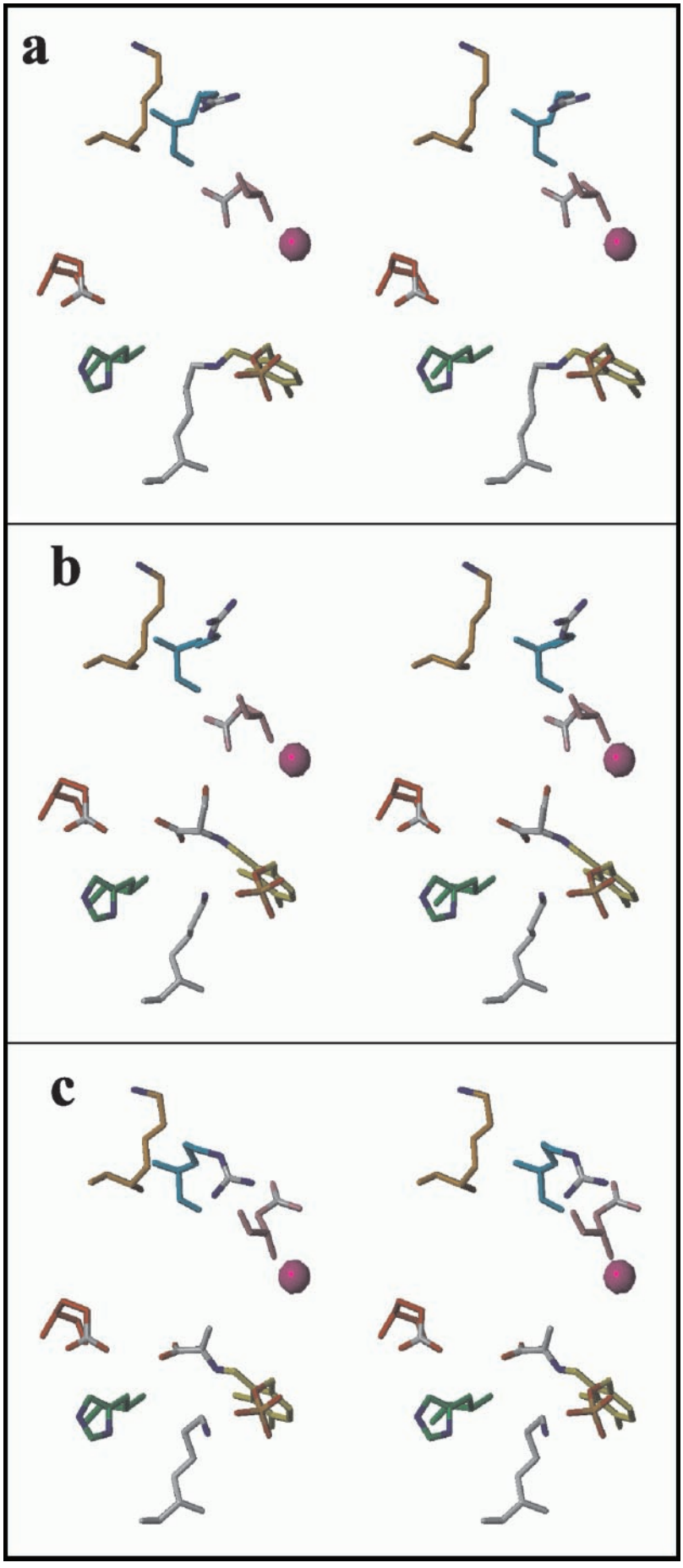

FIG. 7. **Stereoview of the active site of the internal aldimine (*a*), external aldimine (*b*), and α-aminoacrylate (*c*).** The internal aldimine structure was generated from Protein Data Bank code 1kfk (35), the external aldimine from code 1kfj (35), and the aminoacrylate from code 1a5s (12). PLP is displayed in *yellow* with the phosphate group colored by atom type. βLys-87 is *white*; βGlu-109 is *red*; βHis-115 is *green*; βArg-141 is *blue*; βLys-167 is *orange*; βAsp-305 is *pink*; sodium ion is a *violet sphere*. *b* and *c*, L-serine is colored by atom type. Figure was prepared using Sybyl (www.Tripos.com).

7*a*), external aldimine (Fig. 7*b*), and α-aminoacrylate (Fig. 7*c*). In the external aldimine the protonated imidazole ring nitrogen N_{pros} (N^{π}) is at 9.26 and 7.66 Å from the β-hydroxyl and the Cα of serine, respectively, whereas the unprotonated imidazole ring nitrogen N_{tele} (N^{τ}) is at 8.59 and 6.65 Å from the β-hydroxyl and the Cα of serine, respectively. The position of βHis-115 does not change appreciably in the three PLP derivatives. Since no mutant of this residue has been prepared so far, functional data of the enzyme lacking βHis-115 are not available. However, the structural data seem to exclude βHis-115 for any involvement in the catalytic cycle.

βLys-167 is at the periphery of the active site (Fig. 7*a*) and makes a salt bridge with αAsp-56 (not shown) only in the closed state (12, 36). This interaction and the salt bridge between βAsp-305 and βArg-141 were proposed to be relevant for the transmission of allosteric signals between α- and β-active sites (11). The pK_{a3}, determined in the pH dependence of steady-state parameters, was tentatively assigned to βLys-167 (31), and its different state of protonation was possibly associated with the conformational transition between closed and open states (31).

In the internal aldimine, βAsp-305 does not appear to interact with any residue (Fig. 7*a*), whereas in the external aldimine (Fig. 7*b*) the carboxyl group points in the direction of the β-hydroxyl of serine with a distance of 2.76 Å, thus forming a relatively good hydrogen bond (HINT score of 700) only when it is assumed to be deprotonated (the HINT score is 161, assuming a protonated carboxylate). This interaction might stabilize the external aldimine. Furthermore, the carboxylate oxygens are at 4.65–5.97 Å from the α-carbon of L-serine. βAsp-305 is also at 6–9.5 Å from βArg-141, making a very weak interaction (HINT score of 38). Remarkably, in the presence of monovalent cations, the structure of the aminoacrylate intermediate shows that the side chain of βAsp-305 points away from the active site (Fig. 7*c*), being the only residue that significantly changes its position during the β-elimination reaction. In this new position βAsp-305 was suggested to form a salt bridge with βArg-141 (Fig. 7*c*). This new interaction stabilizes the closed form of the aminoacrylate species with respect to the open form of the external aldimine, thus favoring β-elimination. As mentioned earlier, this bond was proposed to be part of the network transmitting intersubunit signals (11). Given this flexibility, a transient position of the carboxyl group closer to the α-carbon of serine cannot be excluded. Furthermore, it should also be reminded that on the basis of the crystallographic data the ionization state of a residue cannot be usually defined except when the distance between residues strongly suggests the formation of a salt bridge or a hydrogen bond. It is also possible to envision that the change in location of the βAsp-305 side chain is associated with a change in the ionization state of the carboxyl group passing from the external aldimine to the aminoacrylate. The pK_{a1} of 6.5, detected by measuring the pH dependence of the steady-state parameters (31), was previously assigned to βAsp-305. Its role was proposed to be the deprotonation of the α-amine of the incoming L-serine and, subsequently, the protonation of the β-hydroxyl group of L-serine (31). The pK_a of Asp-305 might be higher in the open form of the external aldimine where the carboxylate/carboxylic moiety does not form any interaction and lower in the closed form of the aminoacrylate, in the presence of cesium ions, where the carboxylate moiety interacts with β-Arg-141. Recent studies of the βAsp-305 → Ala mutant suggest that βAsp-305 plays a role in the formation of L-serine external aldimine and in the external aldimine-aminoacrylate interconversion (57). However, its key role was proposed to be in the regulation of the conformational equilibrium between open and closed states of the β-subunit (11, 57). In passing from the external aldimine to the aminoacrylate, the interaction with the β-hydroxyl group is lost, and βAsp-305 can swing out to form the salt bridge with βArg-141, stabilizing the closed state (11, 57). The following points were found with βAsp-305 → Ala. (i) The relative stability of the external aldimine and aminoacrylate is altered in favor of the former species. (ii) The β-reaction is 2–14-fold slower depending on the absence or presence of different monovalent ions, with cesium ions partially restoring a wild type steady-state kinetic behavior. (iii) The rate of the β-reaction was slightly faster in the mutant with respect to the wild type, in the presence of the α-subunit ligand glycerol 3-phosphate. (iv) The rate constants for the disappearance of the external aldimine are about 10-fold lower in the mutant with respect to the wild type, both in the absence and presence of cesium and ammonium ions (57).

By combining this wealth of structural and functional data with the pH dependence of the rate constants that were determined in the present work, we propose that the deprotonation of βAsp-305 is associated with pK_{a1}, in agreement with Miles and co-workers (31). However, the role of βAsp-305 might be that of abstracting the proton from the α-carbon. Its location within the active site is compatible with this function. The loss of pK_{a1} in the presence of cesium ions, with and without allosteric effectors, suggests that these ligands stabilize a conformation in which pK_{a1} is shifted to lower values and is therefore undetectable due to protein instability at low pH. The presence of low β-activity in the βAsp-305 → Ala mutant does not contradict this hypothesis because the kinetics of disappearance of the external aldimine is biphasic, thus suggesting that the enzyme possesses two alternative routes of catalysis. Indeed, in the wild type enzyme k_2 was found to account for about 10% of the interconversion to aminoacrylate, with rates that are about 20-fold lower than k_1. This route is essentially unaffected by pH values, monovalent cations, and allosteric effectors (Tables I–II), and might represent a "survival" strategy for TS function. The biphasic decay of the external aldimine to aminoacrylate was also explained to be due to two parallel processes associated with the open and closed states (37). The catalytic role of βAsp-305 is not in contrast with its relevance in the allosteric communication because it further strengthens the coupling between catalysis and regulation. Finally, the pK_a of about 9 that we have detected both in the absence and presence of monovalent cations and α-subunit ligands, and previously observed in the pH dependence of the steady-state parameters of the β-reaction, might be attributed to βLys-87, instead of βLys-167 (31). Only when βLys-87 is charged it can assist the release of the β-hydroxyl group by donating a proton. βLys-87 possesses a location within the active site that is compatible with this catalytic role, and it is a group well suited to exhibit a pK_a close to 9.

Acknowledgments—We thank Dr. Michael Dunn for helpful advice in setting up the rapid scanning stopped-flow apparatus, Dr. Edith Miles for providing us the *E. coli* strain containing the plasmid encoding *S. typhimurium* tryptophan synthase, and Dr. Francesca Spyrakis for the preparation of Fig. 7 and HINT analysis.

REFERENCES

1. Miles, E. W. (1979) *Adv. Enzymol. Relat. Areas Mol. Biol.* **49,** 127–186
2. Miles, E. W. (1991) *Adv. Enzymol. Relat. Areas Mol. Biol.* **64,** 93–172
3. Miles, E. W. (1995) *Subcell. Biochem.* **24,** 207–254
4. Pan, P., Woehl, E., and Dunn, M. F. (1997) *Trends Biochem. Sci.* **22,** 22–27
5. Crawford, I. P. (1960) *Biochim. Biophys. Acta* **45,** 405–407
6. Yanofsky, C., and Crawford, I. P. (1972) in *The Enzymes* (Boyer, P. D., ed) Vol. 7, 3rd Ed., pp. 1–31, Academic Press, New York
7. Dunn, M. F., Aguilar, V., Brzovic, P., Drewe, W. F., Jr., Houben, K. F., Leja, C. A., and Roy, M. (1990) *Biochemistry* **29,** 8598–8607
8. Brzovic, P. S., Sawa, Y., Hyde, C. C., Miles, E. W., and Dunn, M. F. (1992) *J. Biol. Chem.* **267,** 13028–13038
9. Brzovic, P. S., Ngo, K., and Dunn, M. F. (1992) *Biochemistry* **31,** 3831–3839
10. Brzovic, P. S., Hyde, C. C., Miles, E. W., and Dunn, M. F. (1993) *Biochemistry*

32, 10404–10413
11. Ferrari, D., Niks, D., Yang, L. H., Miles, E. W., and Dunn, M. F. (2003) *Biochemistry* **42,** 7807–7818
12. Schneider, T. R., Gerhardt, E., Lee, M., Liang, P. H., Anderson, K. S., and Schlichting, I. (1998) *Biochemistry* **37,** 5394–5406
13. Marabotti, A., De Biase, D., Tramonti, A., Bettati, S., and Mozzarelli, A. (2001) *J. Biol. Chem.* **276,** 17747–17753
14. Osborne, A., Teng, Q., Miles, E. W., and Phillips, R. S. (2003) *J. Biol. Chem.* **278,** 44083–44090
15. Hyde, C. C., Ahmed, S. A., Padlan, E. A., Miles, E. W., and Davies, D. R. (1988) *J. Biol. Chem.* **263,** 17857–17871
16. Faeder, E. J., and Hammes, G. G. (1970) *Biochemistry* **9,** 4043–4049
17. Lane, A. N., and Kirschner, K. (1981) *Eur. J. Biochem.* **120,** 379–387
18. Lane, A. N., and Kirschner, K. (1983) *Eur. J. Biochem.* **129,** 571–582
19. York, S. S. (1972) *Biochemistry* **11,** 2733–2740
20. Goldberg, M. E., York, S., and Stryer, L. (1968) *Biochemistry* **7,** 3662–3667
21. Vaccari, S., Benci, S., Peracchi, A., and Mozzarelli, A. (1996) *Biophys. Chem.* **61,** 9–22
22. Drewe, W. F., Jr., and Dunn, M. F. (1985) *Biochemistry* **24,** 3977–3987
23. Peracchi, A., Mozzarelli, A., and Rossi, G. L. (1995) *Biochemistry* **34,** 9459–9465
24. Hur, O., Niks, D., Casino, P., and Dunn, M. F. (2002) *Biochemistry* **41,** 9991–10001
25. Phillips, R. S. (1991) *Biochemistry* **30,** 5927–5934
26. Schnackerz, K. D., Tai, C. H., Simmons, J. W., III, Jacobson, T. M., Rao, G. S., and Cook, P. F. (1995) *Biochemistry* **34,** 12152–12160
27. Woehl, E. U., and Dunn, M. F. (1995) *Biochemistry* **34,** 9466–9476
28. Goldberg, M. E., and Baldwin, R. L. (1967) *Biochemistry* **6,** 2113–2119
29. Mozzarelli, A., Peracchi, A., Rovegno, B., Dale, G., Rossi, G. L., and Dunn, M. F. (2000) *J. Biol. Chem.* **275,** 6956–6962
30. Lane, A. N., and Kirschner, K. (1983) *Eur. J. Biochem.* **129,** 561–570
31. Ro, H. S., and Miles, E. W. (1999) *J. Biol. Chem.* **274,** 31189–31194
32. Ro, H. S., and Miles, E. W. (1999) *J. Biol. Chem.* **274,** 36439–36445
33. Peracchi, A., Bettati, S., Mozzarelli, A., Rossi, G. L., Miles, E. W., and Dunn, M. F. (1996) *Biochemistry* **35,** 1872–1880
34. Mozzarelli, A., Peracchi, A., Rossi, G. L., Ahmed, S. A., and Miles, E. W. (1989) *J. Biol. Chem.* **264,** 15774–15780
35. Kulik, V., Weyand, M., Seidel, R., Niks, D., Arac, D., Dunn, M. F., and Schlichting, I. (2002) *J. Mol. Biol.* **324,** 677–690
36. Rhee, S., Parris, K. D., Hyde, C. C., Ahmed, S. A., Miles, E. W., and Davies, D. R. (1997) *Biochemistry* **36,** 7664–7680
37. Woehl, E., and Dunn, M. F. (1999) *Biochemistry* **38,** 7118–7130
38. Ruvinov, S. B., Ahmed, S. A., McPhie, P., and Miles, E. W. (1995) *J. Biol. Chem.* **270,** 17333–17338
39. Woehl, E., and Dunn, M. F. (1999) *Biochemistry* **38,** 7131–7141
40. Rhee, S., Parris, K. D., Ahmed, S. A., Miles, E. W., and Davies, D. R. (1996) *Biochemistry* **35,** 4211–4221
41. Weyand, M., Schlichting, I., Herde, P., Marabotti, A., and Mozzarelli, A. (2002) *J. Biol. Chem.* **277,** 10653–10660
42. Marabotti, A., Cozzini, P., and Mozzarelli, A. (2000) *Biochim. Biophys. Acta* **1476,** 287–299
43. Yang, L., Ahmed, S. A., and Miles, E. W. (1996) *Protein Expression Purif.* **8,** 126–136
44. Sam, M. D., and Perona, J. J. (1999) *Biochemistry* **38,** 6576–6586
45. Kellogg, G. E., Semus, S. F., and Abraham, D. J. (1991) *J. Comput. Aided Mol. Des.* **5,** 545–552
46. Kellogg, G. E., and Abraham, D. J. (2000) *Eur. J. Med. Chem.* **35,** 651–661
47. Kellogg, G. E., Burnett, J. C., and Abraham, D. J. (2001) *J. Comput. Aided Mol. Des.* **15,** 381–393
48. Abraham, D. J., and Leo, A. J. (1987) *Proteins* **2,** 130–152
49. Cozzini, P., Fornabaio, M., Marabotti, A., Abraham, D. J., Kellogg, G. E., and Mozzarelli, A. (2002) *J. Med. Chem.* **45,** 2469–2483
50. Fornabaio, M., Cozzini, P., Mozzarelli, A., Abraham, D. J., and Kellogg, G. E. (2003) *J. Med. Chem.* **46,** 4487–4500
51. Burnett, J. C., Botti, P., Abraham, D. J., and Kellogg, G. E. (2001) *Proteins* **42,** 355–377
52. Burnett, J. C., Kellogg, G. E., and Abraham, D. J. (2000) *Biochemistry* **39,** 1622–1633
53. Cozzini, P., Fornabaio, M., Marabotti, A., Abraham, D. J., Kellogg, G. E., and Mozzarelli, A. (2004) *Curr. Med. Chem.* **11,** 1345–1359
54. Drewe, W. F., Jr., and Dunn, M. F. (1986) *Biochemistry* **25,** 2494–2501
55. Weyand, M., Schlichting, I., Marabotti, A., and Mozzarelli, A. (2002) *J. Biol. Chem.* **277,** 10647–10652
56. Fersht, A. (1984) *Enzyme Structure and Mechanism*, 2nd Ed., pp. 155–175, W. H. Freeman & Co., New York
57. Ferrari, D., Yang, L. H., Miles, E. W., and Dunn, M. F. (2001) *Biochemistry* **40,** 7421–7432
58. Dixon, H. B., Clarke, S. D., Smith, G. A., and Carne, T. K. (1991) *Biochem. J.* **278,** 279–284
59. Rhee, S., Miles, E. W., Mozzarelli, A., and Davies, D. R. (1998) *Biochemistry* **37,** 10653–10659
60. Weyand, M., and Schlichting, I. (2000) *J. Biol. Chem.* **275,** 41058–41063
61. Miles, E. W., Kawasaki, H., Ahmed, S. A., Morita, H., and Nagata, S. (1989) *J. Biol. Chem.* **264,** 6280–6287
62. Lu, Z., Nagata, S., McPhie, P., and Miles, E. W. (1993) *J. Biol. Chem.* **268,** 8727–8734
63. Brzovic, P. S., Kayastha, A. M., Miles, E. W., and Dunn, M. F. (1992) *Biochemistry* **31,** 1180–1190
64. Anderson, K. S., Miles, E. W., and Johnson, K. A. (1991) *J. Biol. Chem.* **266,** 8020–8033

pH Dependence of Tryptophan Synthase Catalytic Mechanism: I. THE FIRST STAGE, THE β-ELIMINATION REACTION

Francesca Schiaretti, Stefano Bettati, Cristiano Viappiani and Andrea Mozzarelli

J. Biol. Chem. 2004, 279:29572-29582.
doi: 10.1074/jbc.M401895200 originally published online April 26, 2004
